Synchrotron X-ray study of non-centrosymmetric Tb_3RuO_7 with partial structural disorder

Nobuo Ishizawa,[a]* Tsuyoshi Suwa,[a] Kenji Tateishi[b] and James R. Hester[c]

[a]Ceramics Research Laboratory, Nagoya Institute of Technology, Asahigaoka, Tajimi 507-0071, Japan, [b]Gifu Prefectural Ceramics Research Institute, Tajimi 507-0811, Japan, and [c]Australian National Beamline Facility, KEK, Tsukuba 305-0801, Japan
Correspondence e-mail: ishizawa@nitech.ac.jp

Single-crystal synchrotron X-ray diffraction reveals partial structural disorder of Tb atoms at 293 K in flux-grown Tb_3RuO_7 (triterbium ruthenium heptaoxide) crystals. The structure is noncentrosymmetric and composed of infinite single chains of corner-linked RuO_6 octahedra embedded in a Tb_3O matrix. Two Tb atom sites out of the six crystallographically independent Tb sites are split into two positions. The split sites are separated by approximately 0.3–0.4 Å, with slightly different coordination environments. The RuO_6 octahedra in the present $P2_1nb$ modification have two tilt systems about the a and c axes, in contrast with a single tilt about c in the other $Cmcm$ modifications of Ln_3RuO_7 (Ln = lanthanoid elements).

Comment

The series of Ln_3MO_7 crystals composed of trivalent lanthanide (Ln) and pentavalent transition metal (M = Ru or Os) oxides is known to form $Cmcm$ and $P2_1nb$ modifications. The latter is noncentrosymmetric, with a doubled b length compared with the centrosymmetric $Cmcm$ structure. The two modifications are related by a phase transition, with transition temperatures of 190 K for Sm_3RuO_7, 280 K for Eu_3RuO_7, 235 K for Sm_3OsO_7, 330 K for Eu_3OsO_7 and 430 K for Gd_3OsO_7 (Gemmill et al., 2004, 2005). The $P2_1nb$ modification of Gd_3RuO_7 (Ishizawa et al., 2006) shows a curious structural feature: two Gd atom sites out of the six crystallographically independent positions have relatively large atomic displacement ellipsoids prolate along b. The present paper focuses on Tb_3RuO_7, which has been identified as a new member of the Ln_3RuO_7 structural family for the first time, and deals with the partial structural disorder found in the $P2_1nb$ modification using single-crystal synchrotron X-ray diffraction data collected with a relatively high resolution of $d > 0.42$ Å.

The structure of Tb_3RuO_7 is composed of infinite $[RuO_5]_\infty$ single chains of corner-linked $[RuO_6]$ octahedra embedded in

a matrix of Ln and O atoms, as shown in Fig. 1. There are two crystallographically independent octahedra, viz. $[Ru1O_6]$ and $[Ru2O_6]$, alternately repeated along the chain. The $[Ru1O_6]$ octahedron accommodates two tilt systems of approximately $11°$ about the c axis and $19°$ about the a axis. Although the $[Ru2O_6]$ octahedron is allowed by symmetry to have two tilt systems similar to $[Ru1O_6]$, the tilt about c is negligibly small and it can be considered as having practically only one tilt system of $19°$ about a.

The Ru—O bond distances range from 1.907 (4) to 1.985 (3) Å for Ru1, and from 1.926 (3) to 1.970 (3) Å for Ru2. The mean Ru—O distance is 1.944 Å, which is slightly shorter than that of 1.951 Å in Gd_3RuO_7 (Ishizawa et al., 2006).

Due to the octahedral tilts, the Ru—O—Ru angles along the chain direction differ markedly from $180°$, being 140.8 (2)° for Ru1—O1—Ru2 and 142.3 (2)° for Ru1—O2—Ru2, with a mean value 0.6° smaller than for Gd_3RuO_7. The decrease of Ru—O—Ru angle along the chain provides a closer Ru···Ru intermetallic distance of 3.665 Å. The Ln_3MO_7 structural family is known to possess quasi-one-dimensional conduction along the $[RuO_5]_\infty$ single chains. The conductivity is believed to increase with decreasing Ru···Ru intermetallic distance. For example, the resistivity at room temperature, the mean Ru···Ru distance and the mean Ru—O—Ru angle for Eu_3RuO_7 are 170 Ωcm (Harada & Hinatsu, 2001), 3.706 Å and 143.9°, respectively (Gemmill et al., 2004), while those for Gd_3RuO_7 are 2 Ωcm (Bontchev et al., 2000), 3.692 Å and 142.2°, respectively (Ishizawa et al., 2006). If this is the case in all Ln_3RuO_7 compounds, an enhanced conductivity is expected for Tb_3RuO_7 compared with Gd_3RuO_7.

As described in the refinement section, the Tb5 and Tb6 atom sites in the nonsplit atom model have relatively large atomic displacement ellipsoids prolate along b compared with the other four Tb atoms. The structure can be best described by assuming a split-atom model for these Tb sites (i.e. Tb5a
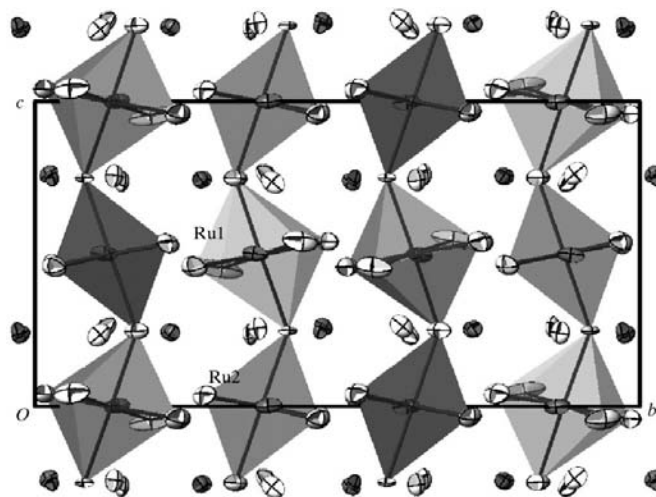

Figure 1
The structure of Tb_3RuO_7, featuring RuO_6 octahedral chains in the Tb (dark grey) and O (light grey) matrix. Displacement ellipsoids are drawn at the 97% probability level (nonsplit atom model). [Symmetry codes: (i) $x + \frac{1}{2}$, $-y + \frac{1}{2}$, $z - \frac{1}{2}$; (ii) $x + \frac{1}{2}$, $-y + 1$, $-z$.]

and Tb5b instead of Tb5, and Tb6a and Tb6b instead of Tb6), as shown in Fig. 2. The distance between Tb5a and Tb5b is 0.322 (5) Å and that between Tb6a and Tb6b is 0.390 (5) Å. These large separation distances indicate that the split-atom model is preferable to the anharmonic vibration model.

The population and coordination numbers differ slightly between these sites. Sites Tb5a and Tb6a are populated with 91.5 (3) and 94.4 (2)% Tb atoms, respectively, and are coordinated by seven O atoms, with Tb—O distances in the range 2.268 (4)–2.556 (3) Å, having a mean of 2.40 Å. The next longer Tb—O distances for these Tb atoms exceed 3.30 Å and can be excluded from the coordination polyhedron. On the other hand, sites Tb5b and Tb6b are much less populated, with 8.5 (3) and 5.6 (2)% occupation by Tb atoms, respectively. They are surrounded by five O atoms, with Tb—O distances in the range 2.197 (6)–2.459 (5) Å, having a mean of 2.30 Å. There are three additional O atoms in the range 2.736 (6)–3.019 (6) Å. Thus, the b sites of atoms Tb5 and Tb6 are considered to have fivefold coordination or perhaps 5+3 coordination. This complicated geometry contrasts with the rather simple coordination of atoms Tb1–Tb4, which are distinctly sevenfold, with the mean Tb—O distances falling in a relatively small range between 2.34 and 2.37 Å. No such disorder was found around the periphery of these Tb atom sites.

We currently have no clear explanation as to why this partial structural disorder occurs at the Tb5 and Tb6 sites. We note, however, two peculiarities associated with these sites. One is that these sites play an important role in the phase transition between $Cmcm$ and $P2_1nb$. There are two crystallographically independent Ln sites in the $Cmcm$ modification, i.e. Ln1 corresponding to Ln1–4 in $P2_1nb$, and Ln2 corresponding to Ln5–6 in $P2_1nb$. The Ln1 site ($Cmcm$) has sevenfold coordination and has little effect on the transition. On the other hand, the Ln2 site ($Cmcm$) has eightfold coordination, and differentiates into sites Ln5 and Ln6 in $P2_1nb$ with sevenfold coordination on the transition. The reduction in coordination is geometrically associated with tilts about c for half of the RuO_6 octahedra. The second peculiarity is the systematic difference between Tb1–4 and Tb5–6 in the bond-valence sums (BVS; Brown, 1992), as given in Table 2. The mean BVS of sites Tb1–Tb4 are 3.18 (11), larger than the

value of 3 that is expected from the formal oxidation state. On the other hand, they show smaller mean values of 2.82 (6) for sites Tb5a and Tb6a, and 2.97 (3) for sites Tb5b and Tb6b.

It would be interesting to determine whether such partial disorder at sites Ln5 and Ln6 is common in all $P2_1nb$ modifications of the Ln_3MO_7 family. Large prolate atomic displacement parameters for Gd5 and Gd6 have been reported in Gd_3RuO_7 (Ishizawa et al., 2006). On the other hand, such a tendency in Ln_3RuO_7 (Ln = Eu and Sm) is less apparent (Gemmill et al., 2004, 2005). It is worth mentioning that such disorder is easily obscured when the resolution of the measurement is reduced. The effect of the resolution level on the results of the refinement has been simulated using the present dataset and is shown in Table 3. The residual electrons around Tb5 and Tb6 decrease from 34 e Å^{-3} ($d > 0.42$ Å) to a negligibly small value of 1 e Å^{-3} ($d > 1.01$ Å) as a function of resolution. Although the prolate feature of the atomic displacement parameters still flags potentially serious problems underlying these sites in all data sets, it is difficult to refine the disordered positions from data taken at low resolution. The resolution should be better than 0.54 Å to distinguish the split-atom model from the single-atom model at a reasonable level of significance.

Experimental

Crystal data

Tb_3RuO_7	$Z = 8$
$M_r = 689.86$	Synchrotron radiation
Orthorhombic, $P2_1nb$	$\lambda = 0.6886$ Å
$a = 10.5672$ (3) Å	$\mu = 34.94$ mm^{-1}
$b = 14.5838$ (3) Å	$T = 293$ K
$c = 7.3453$ (3) Å	$0.05 \times 0.02 \times 0.02$ mm
$V = 1131.98$ (6) Å^3	

Data collection

Photon Factory, Tsukuba; Beamline 14A with four-circle diffractometer	17021 independent reflections
	14382 reflections with $F^2 > 3\sigma(F^2)$
	$R_{int} = 0.017$
Absorption correction: numerical (*ABSORB* in *Xtal3.7*; Hall et al., 2003)	6 standard reflections every 200 reflections intensity decay: corrected by *Xtal3.7* (Hall et al., 2003)
$T_{min} = 0.320$, $T_{max} = 0.546$	
35935 measured reflections	

Refinement

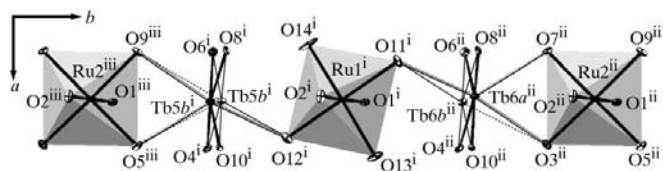|	
$R[F^2 > 2\sigma(F^2)] = 0.018$	$\Delta\rho_{max} = 3.39$ e Å^{-3}
$wR(F^2) = 0.027$	$\Delta\rho_{min} = -2.68$ e Å^{-3}
$S = 1.17$	Absolute structure: Flack (1983), with 7216 Friedel pairs
7216 reflections	Flack parameter: 0.486 (11)
208 parameters	

Figure 2
Geometric relation between the octahedral tilt about c and the interatomic bonds of disordered Tb atoms. The seven bonds around the a site populated by most Tb atoms are drawn with thick lines. The five short bonds and additional two long bonds around the b site populated by trace amounts of Tb atoms are drawn with thin and dashed lines, respectively. [Symmetry codes: (i) $x + \frac{1}{2}, -y + \frac{1}{2}, z - \frac{1}{2}$; (ii) $x + \frac{1}{2}, -y + 1, -z$; (iii) $x + \frac{1}{2}, -y, -z$.]

Table 1
Selected geometric parameters (Å, °).

Tb5a—O6	2.268 (4)	Tb6a—O6	2.323 (4)
Tb5a—O10^i	2.304 (3)	Tb6a—O4^{iii}	2.325 (4)
Tb5a—O8^{ii}	2.321 (3)	Tb6a—O10^{iii}	2.334 (3)
Tb5a—O4^{iii}	2.382 (3)	Tb6a—O8^{iv}	2.352 (3)
Tb5a—O12	2.468 (3)	Tb6a—O11^{iv}	2.465 (3)
Tb5a—O5^{iv}	2.483 (3)	Tb6a—O7	2.486 (3)
Tb5a—O9^{iv}	2.556 (3)	Tb6a—O3	2.517 (3)
Tb5b—O12	2.197 (6)	Tb6b—O4^{iii}	2.208 (5)
Tb5b—O6	2.239 (4)	Tb6b—O10^{iii}	2.214 (5)
Tb5b—O8^{ii}	2.286 (4)	Tb6b—O11^{iv}	2.235 (6)
Tb5b—O10^i	2.330 (4)	Tb6b—O6	2.434 (5)
Tb5b—O4^{iii}	2.405 (4)	Tb6b—O8^{iv}	2.459 (5)
Tb5b—O5^{iv}	2.774 (5)	Tb6b—O3	2.736 (6)
Tb5b—O9^{iv}	2.812 (5)	Tb6b—O7	2.872 (6)
Tb5b—O14	3.019 (6)	Tb6b—O13^{iv}	2.993 (6)
Ru1—O1—Ru2	140.8 (2)	Ru1—O2—Ru2^v	142.3 (2)

Symmetry codes: (i) $x + \frac{1}{2}, -y + \frac{1}{2}, z + \frac{1}{2}$; (ii) $x, y + \frac{1}{2}, -z + \frac{1}{2}$; (iii) $x + \frac{1}{2}, -y + \frac{1}{2}, z - \frac{1}{2}$; (iv) $x, y + \frac{1}{2}, -z - \frac{1}{2}$; (v) $x, y, z + 1$.

Table 2
Bond-valence sums (BVS) for Tb$_3$RuO$_7$.

Atom	BVS	Atom	BVS
Tb1	3.12	Tb5b	2.99
Tb2	3.29	Tb6a	2.78
Tb3	3.05	Tb6b	2.95
Tb4	3.25	Ru1	5.34
Tb5a	2.86	Ru2	5.34

Table 3
Effects of the resolution level on the results of the refinement.

Isotropic atomic displacement parameters for O atoms are assumed in all calculations. d is the resolution level (Å) used in the refinement. N is the number of independent reflections used. R_n is the R factor of the nonsplit model using 133 parameters. $\Delta\rho_n$ is the $\Delta\rho$ (e Å^{-3}) near the Tb5 and Tb6 sites of the nonsplit model. P_n is the maximum prolate ratio of the atomic displacement ellipsoids of Tb5 and Tb6 (nonsplit model). R_s is the R factor of the split model using 144 parameters. $\Delta\rho_s$ is the $\Delta\rho$ (e Å^{-3}) near Tb5/Tb6 of the split model. P_s is the maximum prolate ratio of the atomic displacement ellipsoids of Tb5 and Tb6 (split-atom model).

d (Å)	$\sin\theta/\lambda$	2θ (°)	N	R_n	$\Delta\rho_n$	P_n	R_s	$\Delta\rho_s$	P_s
0.42	1.190	110	7216	0.030	34, 33	3.1	0.020	6.1	2.3
0.45	1.113	100	5982	0.028	27, 26	3.2	0.019	5.4	2.3
0.49	1.027	90	4771	0.026	20, 19	3.4	0.018	4.5	2.4
0.54	0.934	80	3640	0.025	15, 14	4.0	0.017	3.9	2.6
0.60	0.833	70	2623	0.022	9, 9	4.9	0.017	3.0	2.5
0.69	0.726	60	1758	0.020	5, 5	5.2	0.016	2.0	2.8
0.81	0.614	50	1069	0.017	2, 2	5.0	0.023†	6.6†	4.7†
1.01	0.497	40	588	0.017	1, 1	6.9	0.017†	1.2†	3.5†

† The refinement is unstable.

Single-crystal diffraction data were collected using the horizontal-type high-speed four-circle diffractometer at beamline 14A of the Photon Factory, Tsukuba. X-rays of wavelength 0.6886 (1) Å were focused through a pinhole 0.4 mm in diameter on the sample using an Si(111) double-crystal monochromator and a Pt-coated toroidal mirror. The wavelength was calibrated by a spherical Si standard crystal 75 μm in diameter. Dispersion and absorption coefficients at this wavelength were taken from tables given by Sasaki (1989, 1990). An eight-channel avalanche photodiode detector was used for photon counting (Kishimoto *et al.*, 1998). Since the detector has a counting linearity above 10^9 counts per second, neither absorbers nor attenuators were employed. The *Xtal3.7* program package was used for further calculations (Hall *et al.*, 2003).

The least-squares refinement applying anisotropic atomic displacement parameters for all fully populated atom sites yielded R/R_w factors of 0.027/0.039 for 7216 reflections. However, large residual electron-density peaks of 33–34 e Å^{-3} were found about 0.42 Å from both Tb5 and Tb6 in the difference Fourier map after the refinement. Further refinement to examine the population of Tb and Ru atom sites did not significantly affect the R/R_w factors or the residual electron-density peaks. The deviation of the populations from 100% was marginal. A split-atom model for Tb5 into Tb5a and Ta5b, and for Tb6 into Tb6a and Tb6b, was then undertaken. The refinement decreased the R/R_w factors to 0.017/0.027 for 7216 independent reflections and 208 parameters. Thus, this model was adopted according to Hamilton's significance test [*International Tables for Crystallography* (2004), Vol. C, pp. 703–704]. The residual electron density near Tb5 and Tb6 decreased to less than 3.5 e Å^{-3}. The refined Flack (1983) parameter of nearly 50% suggested the presence of very fine micro-twins related by an inversion operation, as is common for most $P2_1nb$ modifications of Ln$_3$RuO$_7$ and Ln$_3$OsO$_7$. These twins were supposedly introduced by the phase transition from the centrosymmetric base-centred lattice to the noncentrosymmetric primitive lattice with doubled cell volume, allowing the generation of eight possible variants at room temperature.

The refinement with anisotropic atomic displacement parameters for all atoms revealed a prolate feature for O14. The isotropic atomic displacement parameter of O14 was normal compared with the other O atoms. No significant residual electrons were found near O14 before or after refinement assuming anisotropic atomic displacement parameters. Therefore, the prolate feature of O14 could be an artifact that occurred during the least-squares procedure.

Data collection: *BL14A* diffractometer control software (Satow *et al.*, 2005); cell refinement: *LATCON* in *Xtal3.7* (Hall *et al.*, 2003); data reduction: *DIFDAT*, *ABSORB*, *SORTRF* and *ADDREF*, all in *Xtal3.7*; program(s) used to solve structure: *Xtal3.7*; program(s) used to refine structure: *CRYLSQ* in *Xtal3.7*; molecular graphics: *ATOMS* (Dowty, 2005); software used to prepare material for publication: *BONDLA* and *CIFIO*, both in *Xtal3.7*.

Supplementary data for this paper are available from the IUCr electronic archives (Reference: SQ3070). Services for accessing these data are described at the back of the journal.

References

Bontchev, R. P., Jacobson, A. J., Gospodinov, M. M., Skumryev, V., Popov, V. N., Lorenz, B., Meng, R. L., Litvinchuk, A. P. & Iliev, M. N. (2000). *Phys. Rev. B*, **62**, 12235–12240.
Brown, I. D. (1992). *Acta Cryst.* B**48**, 553–572.

inorganic compounds

Dowty, E. (2005). *ATOMS for Windows*. Version 6.2. Shape Software, 521 Hidden Valley Road, Kingsport, TN 37663, USA. URL: http://www.shape-software.com.

Flack, H. D. (1983). *Acta Cryst.* A**39**, 876–881.

Gemmill, W. R., Smith, M. D., Mozharivsky, Y. A., Miller, G. J. & zur Loye, H.-C. (2005). *Inorg. Chem.* **44**, 7047–7055.

Gemmill, W. R., Smith, M. D. & zur Loye, H.-C. (2004). *Inorg. Chem.* **43**, 4254–4261.

Hall, S. R., du Boulay, D. J. & Olthof-Hazekamp, R. (2003). Editors. *Xtal3.7 System*. University of Western Australia, Australia. URL: http://xtal.sourceforge.net/

Harada, D. & Hinatsu, Y. (2001). *J. Solid State Chem.* **158**, 245–253.

Ishizawa, N., Hiraga, K., du Boulay, D., Hibino, H., Ida, T. & Oishi, S. (2006). *Acta Cryst.* E**62**, i13–i16.

Kishimoto, S., Ishizawa, N. & Vaalsta, T. P. (1998). *Rev. Sci. Instrum.* **69**, 384–391.

Sasaki, S. (1989). KEK Report 88-14, 1–136. KEK, 1-1 Oho, Tsukuba 305-8001, Japan.

Sasaki, S. (1990). KEK Report 90-16, 1–143. KEK, 1-1 Oho, Tsukuba 305-8001, Japan.

Satow, Y., Hester, J. R. & Vaalsta, T. P. (2005). *DIFF14A*. Unpublished.